Empirical modeling and simulation of phase noise in long-haul coherent optical transmission systems

Maurizio Magarini,[1,*] Arnaldo Spalvieri,[1] Francesco Vacondio,[2] Marco Bertolini,[3] Marianna Pepe,[3] and Giancarlo Gavioli[3]

[1]*Dipartimento di Elettronica e Informazione, Politecnico di Milano, Piazza L. da Vinci 32, 20133 Milano, Italy*
[2] *Alcatel-Lucent Bell Labs, Route de Villejust, 91620 Nozay, France*
[3] *Alcatel-Lucent Italia, Via Trento 30, 20871 Vimercate, Italy*
[*]*magarini@elet.polimi.it*

Abstract: An empirical phase noise channel model suitable for performance evaluation of high spectrally efficient modulations in 100G long-haul coherent optical transmission systems using polarization-division multiplexed and wavelength-division multiplexing channels is presented. The derivation of the model is worked out by exploiting the similarity between the power spectral density of the carrier extracted from the analysis of propagation measurements and the Lorentzian spectrum that is usually adopted to describe instabilities of semiconductor lasers. The proposed channel model is characterized by only two parameters: the linewidth of the carrier and the signal-to-noise ratio. We show that in the case of quadrature phase-shift keying transmission a good agreement exists between quantitative measures of performance extracted by processing experimental data and those obtained from simulations based on the use of the empirical model.

OCIS codes: (060.1660) Coherent communications; (060.4510) Optical communications; (060.5060) Phase modulation; (190.4975) Parametric processes.

References and links

1. S. J. Savory, G. Gavioli, R. I. Killey, and P. Bayvel, "Electronic compensation of chromatic dispersion using a digital coherent receiver," Opt. Express **15**(5), 2120–2126 (2007), http://www.opticsinfobase.org/abstract.cfm?URI=oe-15-5-2120.
2. I. B. Djordjevic, M. Arabaci, and L. L. Minkov, "Next generation FEC for high-capacity communication in optical transport networks," J. Lightwave Technol. **27**(16), 3518–3530 (2009).
3. F. Chang, K. Onohara, and T. Mizuochi, "Forward error correction for 100 G transport networks," IEEE Commun. Mag. **48**(3), S48–S55 (2010).
4. C. Herzet, N. Noels, V. Lottici, H. Wymeersch, M. Luise, M. Moeneclaey, and L. Vandendorpe, "Code-aided turbo synchronization," Proc. IEEE **95**(6), 1255–1271 (2007).
5. A. Barbieri, G. Colavolpe, and G. Caire, "Joint Iterative Detection and Decoding in the Presence of Phase Noise and Frequency Offset," IEEE Trans. Commun. **55**(1), 171–179 (2007).
6. R. W. Tkach and A. R. Chraplyvy, "Phase noise and linewidth in an InGaAsP DFB laser," J. Lightwave Technol. **4**(11), 1711–1716 (1986).
7. G. J. Foschini and G. Vannucci, "Characterizing filtered light waves corrupted by phase noise," IEEE Trans. Inf. Theory **34**(6), 1437–1448 (1988).
8. K. P. Ho, *Phase-Modulated Optical Communication Systems*, (Springer-Verlag, New York, NY, 2005).
9. A. P. T. Lau and J. M. Kahn, "Signal design and detection in presence of non-linear phase noise," J. Lightwave Technol. **25**(10), 3008–3016 (2007).
10. A. Bononi, N. Rossi, and P. Serena, "Transmission limitations due to fiber nonlinearity," in *Optical Fiber Communication Conference and Exposition*, OSA Technical Digest (CD) (Optical Society of America, 2011), paper OWO7.
11. Z. Tao, W. Yan, L. Liu, L. Li, S. Oda, T. Hoshida, and J. C. Rasmussen, "Simple fiber model for determination of XPM effects," J. Lightwave Technol. **29**(7), 974–986 (2011).
12. M. Murakami and S. Saito, "Evolution of field spectrum due to fiber-nonlinearity-induced phase noise in in-line optical amplifier systems," IEEE Photon. Technol. Lett. **4**(11), 1269–1272 (1992).

#151424 - $15.00 USD Received 20 Jul 2011; revised 9 Sep 2011; accepted 16 Sep 2011; published 24 Oct 2011

13. Z. Tao, L. Li, L. Liu, W. Yan, H. Nakashima, T. Tanimura, S. Oda, T. Hoshida, and J. C. Rasmussen, "Improvements to digital carrier phase recovery algorithm for high-performance optical coherent receivers," IEEE J. Select. Top. Quantum Electron. **16**(5), 1201–1209 (2010).
14. A. Demir, A. Mehrotra, and J. Roychowdhury, "Phase noi**se** in oscillators: a unifying theory and numerical methods for characterization," IEEE Trans. Circuits Syst., I Fundam. Theory Appl. **47**, 655–674 (2000).
15. J.-C. Antona, M. Lefrançois, S. Bigo, and G. Le Meur, "Investigation of advanced dispersion management techniques for ultra-long haul transmissions," in *Proceedings of European Conference on Optical Communications*, Glasgow, Scotland, 2005, Mo.3.2.6.
16. M. Salsi, C. Koebele, P. Tran, H. Mardoyan, E. Dutisseuil, J. Renaudier, M. Bigot-Astruc, L. Provost, S. Richard, P. Sillard, S. Bigo, and G. Charlet, "Transmission of 96×100Gb/s with 23% Super-FEC Overhead over 11,680km, using Optical Spectral Engineering," in *Optical Fiber Communication Conference*, OSA Technical Digest (CD) (Optical Society of America, 2011), paper OMR2. *http://www.opticsinfobase.org/abstract.cfm?URI=OFC-2011-OMR2*
17. T. Mizuochi, Y. Miyata, K. Kubo, T. Sugihara, K. Onohara, and H. Yoshida, "Progress in soft-decision FEC," in *National Fiber Optic Engineers Conference*, OSA Technical Digest (CD) (Optical Society of America, 2011), paper NWC2. *http://www.opticsinfobase.org/abstract.cfm?URI=NFOEC-2011-NWC2*
18. U. Mengali and A. N. D'Andrea, *Synchronization Techniques for Digital Receivers*, (Plenum Press, New York, NY, 1997).
19. T. Pfau, S. Hoffmann, and R. Noe, "Hardware-efficient coherent digital receiver concept with feedforward carrier recovery for M-QAM constellations," J. Lightwave Technol. **27**(8), 989–999 (2009).

1. Introduction

Polarization division multiplexed (PDM) transmissions with coherent detection of spectrally efficient modulation formats and digital signal processing (DSP) represent the enabling technologies to meet the demand for high capacity required by next generation wavelength-division multiplexing (WDM) long-haul optical transport networks [1]. Together with the development of advanced DSP algorithms for coherent demodulation and detection, the introduction of forward error correction (FEC) coding schemes, with overheads in the order of 20 percent that are based on soft decision decoding and iterative decoding, and their combination with high-order modulation formats is a subject of intense research activities [2,3]. Because of the challenge of capacity-approaching coded modulation schemes with such overhead rates, the operating signal-to-noise ratio (SNR) results to be much lower than that of actual coded systems based on hard decision decoding with a standard 7 percent FEC overhead. As it is well known, at such low SNR values carrier synchronization can become a limiting issue [4,5].

One of the main drawbacks of coherent detection for high-order modulation formats at low SNR is represented by their sensitivity to phase noise. In the case of linear propagation, carrier phase noise is dominated by laser phase noise and performance degradation due its effects is commonly evaluated by using a Wiener process model [6,7]. When nonlinear phase noise (NLPN) induced by the interaction of the signal and amplified spontaneous emission (ASE) noises through the Kerr effect is considered, the performance can be evaluated analytically by resorting to methods that are based on the physical description of the propagation [8,9]. A statistical characterization of NLPN allowing for analytical performance evaluation of phase modulated signals is given in [8]. The knowledge of the joint probability density function (pdf) of the amplitude and phase of the received signal has been exploited in [9] to derive the analytical expressions of the maximum-likelihood decision boundaries associated to the received phase-shift keying (PSK) signal constellation and the relative performance.

It is worth emphasizing that the analysis in [8] has been derived for the case of single-polarization by taking into consideration only the nonlinearities induced by the interaction of the signal with ASE noise in its bandwidth and in the adjacent channel bandwidths, but without considering the waveform distortion caused by neighboring interfering channels. Simulation results that are reported in [10] show that for WDM transmission with a central PDM quadrature phase shift keying (QPSK) test channel NLPN induced by the nonlinear interaction between signal and ASE is a second order effect in determining the entity of nonlinear impairments, both for the case of homogeneous transmission and for that of hybrid transmission. Specifically, in [10] it is shown that in WDM systems cross-nonlinearities give rise to interactions of neighboring channels according to their power level and their state of polarization. In the case of homogeneous transmission cross-polarization modulation

#151424 - $15.00 USD Received 20 Jul 2011; revised 9 Sep 2011; accepted 16 Sep 2011; published 24 Oct 2011

dominates over nonlinear signal-noise interactions while in the hybrid case the cross-phase modulation is almost entirely due to the modulation-induced large intensity excursion of adjacent channels. A simplified analytical model has been recently derived in [11] to ease the evaluation of nonlinear effects due to both the cross-polarization modulation and the cross-phase modulation induced by adjacent channels. Although the analytical model presented in [11] has the advantage of avoiding the time-consuming computation associated to the split step Fourier method, it does not provide any statistical characterization of the received random carrier phase process in terms of amplitude distribution and power spectral density.

Due to the inherent difficulties associated to the analysis when many nonlinear effects are considered, no special attention seems to have been given to the spectral characterization of the carrier phase noise in the existing literature. As a matter of fact, it is known that the spectral line subject to NLPN experiences a spectral distortion [12]. Two important factors for the design of carrier phase recovery circuits are the linewidth of the carrier phase noise and the level of ASE that is proportional to the inverse of the SNR [13]. The development of models that are able to capture and reproduce the effects at the SNR values of interest would allow us to evaluate the performance by running fast simulation programs that does not require off-line processing of data extracted from lab experiments or the physical description of the propagation. A challenge in optical channel modeling is the translation of a detailed physical propagation model into a form that is suitable for simulation. In contrast, parametric models based on measured data allow for an empirical description of the carrier phase-noise in time and in frequency domain. The characterization of the underlying random processes and power spectra are obtained by fitting model parameters to measured data.

In this paper an empirical power spectral density characterization of the carrier phase noise after nonlinear propagation is derived. We show that the Wiener model is still adequate to describe carrier phase noise effects at SNR values that are of interest for soft-decision decoding of a 100G PDM-QPSK WDM channel after nonlinear propagation in different transmission scenarios. The effectiveness of the model is demonstrated by proving that the performance obtained from simulations based on the use of the empirical Wiener model fits the performance extracted by processing experimental data. Numerical results are presented for a 50 GHz spaced WDM grid where a central 100 Gb/s PDM-QPSK test channel is co-propagated either with "hybrid" neighboring 10 Gb/s on-off keying (OOK) channels or with "homogeneous" 50 Gb/s PDM-QPSK channels along standard single-mode optical fiber (SSMF) and nonzero dispersion shifted fiber (NZDSF) with recirculating loops. The length of the optical links considered for different transmission scenarios are comprised between 900 and 1800 km. These have been set by the maximum reach associated to the SNR at which corresponds a target bit-error rate (BER) of 10^{-2}, a typical value for the performance measured at the input of the soft decoder when overheads in the order of 20 percent are considered. A main finding is the experimental evidence that the linewidth associated to the carrier phase noise after propagation exhibits a broadening compared to its nominal value defined by the transmitting and receiving lasers. In the case of hybrid transmission a larger broadening has been observed compared to that of homogeneous transmission.

2. Empirical system model

The discrete time empirical model we consider for the *k*-th sample of the signal at the input of the carrier phase recovery circuit is

$$x_k = s_k \cdot e^{j\theta_k} + n_k, \tag{1}$$

where $\{s_k\}$ is the sequence of QPSK transmitted symbols with unitary average power and $\{n_k\}$ is a zero mean complex additive white Gaussian noise (AWGN) sequence with variance σ_n^2.

#151424 - $15.00 USD Received 20 Jul 2011; revised 9 Sep 2011; accepted 16 Sep 2011; published 24 Oct 2011

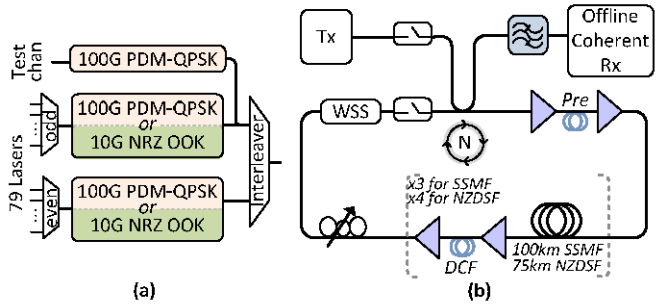

Fig. 1. Experimental set-up for (a) generation, and (b) transmission and coherent detection of 100G homogeneous and hybrid WDM transmission.

The unknown time-varying phase of the incoming carrier is modeled as a Wiener process

$$\theta_{k+1} = \theta_k + \delta \cdot w_k, \tag{2}$$

where δ is a constant and $\{w_k\}$ is a sequence of real independent and identically distributed Gaussian random variables with zero mean and unitary variance. For small δ, the spectrum of the continuous-time complex exponential $e^{j\theta(t)}$ affected by random phase walk that generates the sampled carrier sequence $e^{j\theta k}$ is the Lorentzian function [14]

$$L_\theta(f) = \frac{4\delta^2 T}{\delta^4 + 16\pi^2 f^2 T^2}, \tag{3}$$

where T is the symbol interval. The Lorentzian function is often characterized by its half-width at half-maximum (HWHM) frequency

$$f_{HWHM} = \frac{\delta^2}{4\pi T}. \tag{4}$$

The effect of the modulation is easily removed from the received signal in Eq. (1) by multiplication for s_k^* to obtain

$$c_k = x_k \cdot s_k^* = e^{j\theta_k} + n_k', \tag{5}$$

where n_k' is statistically equivalent to n_k and * denotes complex conjugation. For small δ, carrier aliasing can be neglected and the power spectrum of the signal in Eq. (5) can be approximated as

$$S_c(f) \approx \frac{1}{T} L_\theta(f) + \frac{1}{\mathrm{SNR}}, \quad -\frac{1}{2} \le fT < \frac{1}{2} \tag{6}$$

where SNR=$1/\sigma_n^2$ is the signal-to-noise ratio. From Eq. (1), Eq. (2) and Eq. (6) one observes that the empirical channel model can be completely specified once the values of the two parameters δ and SNR are known. The procedure used to extract the two parameters from experimental data is described in section 4.

3. Experimental setup and receiver processing

The experimental setup for signal generation is shown in Fig. 1(a). A laser source at 1545 nm was modulated using an integrated dual-polarization nested Mach-Zehnder modulator to generate a 100 Gb/s PDM-QPSK signal. Two WDM transmission configurations are tested; in

#151424 - $15.00 USD Received 20 Jul 2011; revised 9 Sep 2011; accepted 16 Sep 2011; published 24 Oct 2011

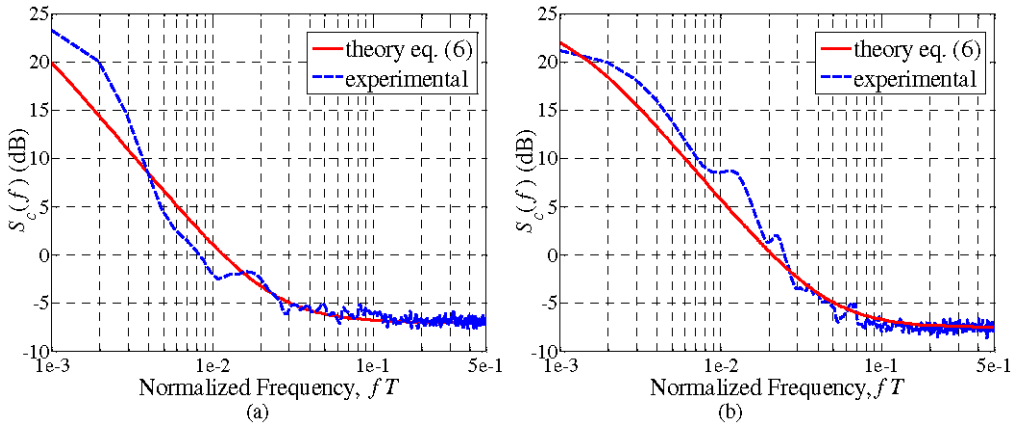

Fig. 2. Spectrum of the carrier plus AWGN for the empirical model and for the experimental data. (a) homogeneous case; (b) hybrid case.

the hybrid transmitter configuration the test channel is wavelength multiplexed with 79 OOK non-return-to-zero (NRZ) channels modulated at 10 Gb/s spaced at 50 GHz; in the homogeneous transmission configuration the test channel is multiplexed with 79 PDM-QPSK 100G channels spaced at 50 GHz. The same distributed-feedback (DFB) laser with nominal f_{HWHM}=500 kHz was used as a light source for the test and the interfering channels. According to Eq. (4) this linewidth corresponds to $\delta = 1.5 \cdot 10^{-2}$.

The signal was then launched into the recirculating loop depicted in Fig. 1(b). The loop consisted of 3×100 km SSMF compensated spans, or 4×75 km compensated spans of NZDSF. The loop included a dual-stage erbium doped fiber amplifiers (EDFAs) per span, a polarization scrambler, and a wavelength selective switch (WSS) filter for power equalization. A dispersion compensation fiber (DCF) is used between the two-stage EDFAs for partial dispersion compensation, according to a dispersion map for typical terrestrial systems [15]. The power at EDFA output was optimized for maximum reach, *i.e.*, for optimal balance of amplified spontaneous emission noise and fiber nonlinearities. The maximum reach at BER target lower than $2 \cdot 10^{-2}$ for homogeneous WDM transmission was found to be 6 SSMF loops and 5 NZDSF loops, while for hybrid WDM transmission was found to be 5 SSMF loops and 3 NZDSF loops. The launch powers into the SSMF and NZDSF were −1 dBm/channel and −3 dBm/channel for homogeneous transmission and −2 dBm/channel and −7 dBm/channel for heterogeneous transmission, respectively. Note that, a target BER at the input of the decoder in the order of 10^{-2} is usually considered for soft-decision decoding with rates in the order of 20 percent [3,16,17]. At the receiver, the signal was selected by an optical filter, passed through a polarization beam splitter and then combined with the local oscillator via two optical 90 degree hybrids to select the in-phase and quadrature components of the two polarizations. Since the local oscillator laser is of the same type as that used at the transmitter, the back-to-back (B2B) nominal linewidth of the cascade of the transmitting and receiving oscillators turns out to be f_{HWHM} = 1 MHz. On conversion into the electrical domain, the signal was digitized at 50 GSa/s using a real-time sampling scope with a bandwidth of 16 GHz. The sampled waveforms were then processed offline in a conventional PC. The receiver DSP is as described in [1].

4. Experimental data analysis

In this section the procedure used to match the spectrum of the empirical model introduced in section 2 with that of the channel extracted from the measured data is described and a comparison of their performance is done. Results are shown for the power spectra, the phase mean-square error (MSE) between the recovered carrier and the incoming carrier phase, and the BER and the distribution of the errors after coherent QPSK differential decoding.

#151424 - $15.00 USD Received 20 Jul 2011; revised 9 Sep 2011; accepted 16 Sep 2011; published 24 Oct 2011

Table 1. BER and MSE_θ measures extracted from the experimental data and those obtained by simulation using the empirical model

	Homogeneous				Hybrid			
	SSMF		NZDF		SSMF		NZDF	
	BER	MSE_θ	BER	MSE_θ	BER	MSE_θ	BER	MSE_θ
Experimental	$3.52\cdot10^{-2}$	$1.81\cdot10^{-2}$	$3.56\cdot10^{-2}$	$1.98\cdot10^{-2}$	$3.04\cdot10^{-2}$	$1.39\cdot10^{-2}$	$4.31\cdot10^{-2}$	$2.74\cdot10^{-2}$
Empirical	$3.28\cdot10^{-2}$	$1.72\cdot10^{-2}$	$3.61\cdot10^{-2}$	$1.95\cdot10^{-2}$	$3.02\cdot10^{-2}$	$1.41\cdot10^{-2}$	$4.44\cdot10^{-2}$	$2.94\cdot10^{-2}$

A practical procedure is used for fitting the spectrum of the empirical model defined in Eq. (6) to that of measured data. The first step consists in generating the signal of Eq. (5) for the experimental data. This is done by analyzing the signal at the output of the constant modulus algorithm (CMA) for each considered propagation scenario and beating it with the known transmitted data symbols. Data aided maximum likelihood carrier frequency estimation is used to remove any frequency offset after the CMA equalizer [18]. The tuning of the two parameters δ and SNR is done to have the best possible match between the resulting power spectrum and that defined in Eq. (6). Figure 2(a) shows the spectra of the carrier plus AWGN extracted from experimental data in the case of SSMF homogeneous transmission and that obtained using the values SNR = 7 dB and $\delta = 6.6\cdot10^{-2}$. Such a δ corresponds to $f_{\mathrm{HWHM}} \approx 10$ MHz, thus evidencing an expansion of a factor 10 compared to the nominal B2B linewidth. Figure 2(b) shows the same spectra in the case of NZDSF hybrid transmission where the values are SNR = 7.3 dB and $\delta = 1.25\cdot10^{-1}$. In this case a huge broadening is observed compared to the homogeneous case with $f_{\mathrm{HWHM}} \approx 35$ MHz. From the Figures we can clearly distinguish between the contribution of the $1/f^2$ Lorentzian spectrum associated to the carrier and the one of the white spectrum of the Gaussian noise with amplitude 1/SNR. Similar results could be shown for the other two propagation scenarios where the values obtained for the fitting parameters are SNR = 6.9 dB and $\delta = 7.2\cdot10^{-2}$, for NZDSF homogeneous transmission, and SNR = 7.8 dB and $\delta = 1.35\cdot10^{-1}$, for SSMF hybrid transmission, respectively.

The phase MSE of the coherent demodulator is defined as

$$\mathrm{MSE}_{\vartheta} = E\left\{\left[\left(\hat{\theta}_k - \theta_k\right)_{\mathrm{mod}\,\pi/2}\right]^2\right\}, \tag{7}$$

where $E\{\cdot\}$ is the expectation, $\mathrm{mod}\pi/2$ is the modulo $\pi/2$ operation and $\hat{\vartheta}_k$ is the estimated phase. Due to the four-fold rotationally symmetry of the QPSK constellation, the recovered phase differs of an integer multiple of $\pi/2$ from the true carrier phase. This problem is commonly tackled by differentially encoding the bits associated to the constellation points. The BER is computed after coherent demodulation followed by differential decoding at the receiver. Carrier phase recovery after carrier frequency compensation implements the non-data aided approximated maximum likelihood algorithm of [19] where the length of the post-detection filter is optimized to minimize the BER. Table 1 reports the estimates of the considered performance measures obtained by computer simulations for all the considered transmission scenarios. Numerical results for experimental data have been obtained by averaging over multiple acquisitions. For the empirical model, the same parameters SNR and δ mentioned above were used.

To further validate the empirical model, in Fig. 3(a) and Fig. 3(b) are reported the estimated pdfs of the inter-arrival time between two consecutive errors after differential decoding for the two considered transmission scenarios. We observe that also in this case the empirical model is able to closely reproduce the measure extracted from experimental data.

The validity of the model was also verified for the same scenarios at other SNR values extracted from the measurements. It is worth noting that, while in the hybrid transmission case, for the same scenario, a change in the relative contribution of the received carrier

#151424 - $15.00 USD Received 20 Jul 2011; revised 9 Sep 2011; accepted 16 Sep 2011; published 24 Oct 2011

linewidth to the power spectral density was observed, no significant variations were found for the homogeneous cases.

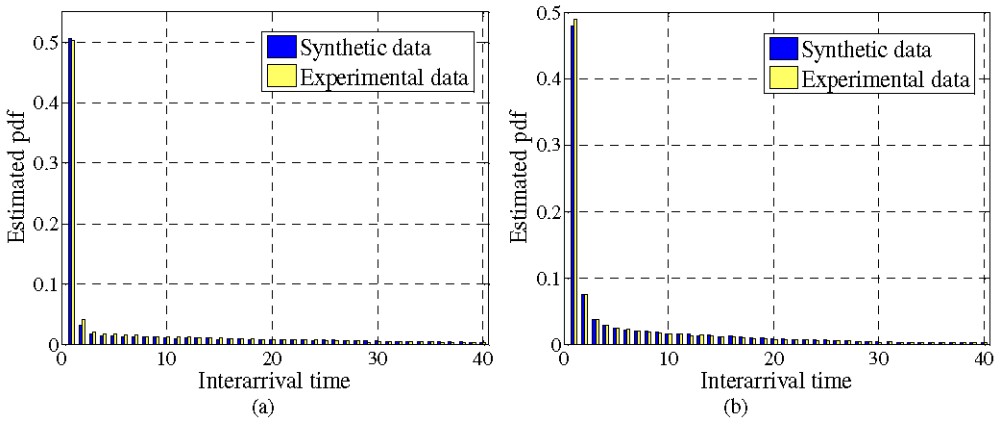

Fig. 3. Distribution of inter-arrival time between two consecutive errors after differential QPSK decoding. (a) homogeneous transmission; (b) hybrid transmission case.

5. Conclusion

An empirical phase noise channel model suitable for reproducing fiber's nonlinearity effects on carrier phase noise at SNR values that are of interest for soft decision decoding in 100G PDM-WDM long-haul coherent optical transmission systems has been presented. Imposing the model of random phase walk plus AWGN, the channel is described by only two parameters: the value of δ, defining the linewidth of the Wiener phase noise, and the SNR of the AWGN. A major finding is that the experimental data worked out for several channel conditions are well fitted by the proposed channel model. Moreover, a broadening of the linewidth of the received carrier phase noise is observed compared to its nominal value defined by the back-to-back transmission where only the contribution of the lasers is present. As a matter of fact, a larger broadening has been observed in the case of hybrid transmission than in that of homogeneous transmission. To claim the fit between the empirical model and the experimental data, we have considered

- carriers' spectrum plus noise floor;
- phase MSE;
- BER and distribution of the errors after coherent demodulation followed by differential QPSK decoding.

Since the proposed empirical channel model is able to reproduce the same effects of experiments on the transmitted data, it is possible to replace the conventional short pseudorandom sequences that are used in lab experiments to produce the received sequence for offline processing with longer pattern sequences produced by the error correcting code. This allows for an easier performance evaluation of coded modulation schemes at the BER of interest completely within a simulation domain.

Acknowledgments

The authors would like to thank P. Boffi and P. Martelli of Dipartimento di Elettronica e Informazione at Politecnico di Milano for useful discussions and feedbacks on this work.

#151424 - $15.00 USD Received 20 Jul 2011; revised 9 Sep 2011; accepted 16 Sep 2011; published 24 Oct 2011